Diels–Alder Cyclization of a Dihydropyridine: NMR Spectroscopy, X-Ray Crystallography, and DFT Computations. Bent Aromatic Dimeric Clusters in the Solid Phase

by **Gideon Fraenkel***, **Jinhua Song**, **Albert Chow**, and **Judith C. Gallucci**

Department of Chemistry, Ohio State University, 100 W. 18th Avenue, Columbus, OH 43210, USA (phone: +1-614-2924210; fax: +1-614-2921685; e-mail: fraenkel@mps.ohio-state.edu)

Structural studies of the *N*-(2,4-dinitrophenyl) derivative of a *Diels–Alder*-cyclized 1,2-dihydropyridine both unequivocally established the polycyclic framework and revealed interesting distortions of aromatic structure and unique dimeric clustering of the aromatic entities in the solid state.

Introduction. – We have previously shown that, whereas mixtures of pyridines **1** with *Grignard* reagents remain unchanged over several weeks at room temperature, addition of ClCOOEt immediately gave the 1,2-dihydro-1-(ethoxycarbonyl)pyridine **2** (see *Scheme 1* [1a]).

Scheme 1

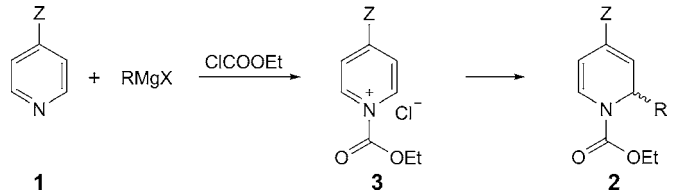

Evidently, ClCOOEt reacts much faster with the N-atom of pyridine than with the *Grignard* reagent. Then, the *Grignard* reagent adds rapidly to the resulting electron-deficient pyridinium salt **3** [1b][1c]. In a similar fashion, we reported that acylation of the (pyridin-4-yl)alkylmagensium chloride **4** with ClCOOEt takes place at the N-atom (see **5**), immediately followed by ring closure to the spiro-dihydropyridine **6** [2] (*Scheme 2*). Again, the N-atom of pyridine is more reactive to acylation than the *Grignard* reagent.

Scheme 2

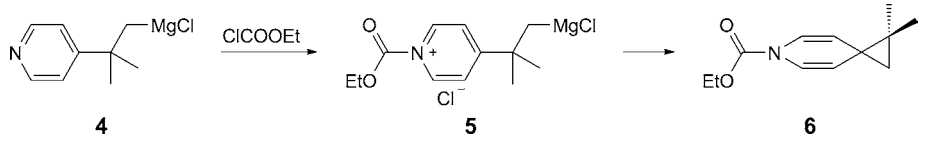

It has also been reported that 2-alkenyl-1-(alkoxycarbonyl)-1,2-dihydropyridines **7**, prepared using the reaction shown in *Scheme 1*, easily undergo intramolecular *Diels–Alder* reactions (see **7** → **8**; *Scheme 3*).

Scheme 3

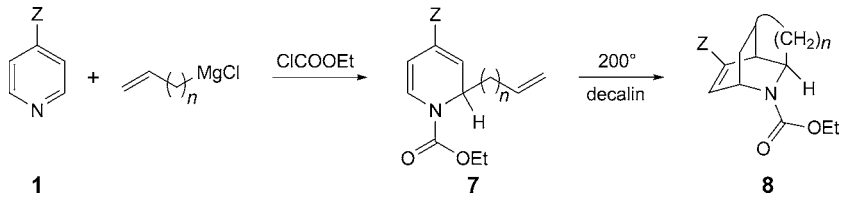

Structures were assigned as consistent with the NMR data, together with the assumed course of the chemistry [3]. In our experience and as shown below, NMR spectra of cycloadducts of type **8** are quite complicated and not necessarily unambiguously definitive of the expected reaction products. Hence, considering that reactions such as **1** → **7** → **8** are potentially highly efficient routes to complex polycyclic analogs of aza-alkaloids and of potential pharmacological application, we studied the *Diels–Alder* cyclization of a new similar system in considerable detail.

Below, we show how X-ray crystallography is indispensable to identify the structures of compounds of type **8**. Further computations of chemical shifts using B3LYP/6-311G* in conjunction with GIAO closely reproduced the observed values, thus validating the DFT model for our *Diels–Alder* product and at the same time assigning the previously ambiguous shifts.

Results and Discussion. – *Synthesis.* In the course of some new studies of ion-pairing within and among dihydropyridine salts [4], we investigated the *Diels–Alder* reactions of 1-(alkoxycarbonyl)-4-alkyl-1,2-dihydro-2-(pent-2-enyl)pyridines. The precursors, **9a**, **9b**, and **9c** (*Scheme 4*), were prepared as depicted in *Scheme 1*. Their structures were confirmed unambiguously by the NMR data. These compounds appear to consist of almost 1 : 1 mixtures of rotamers around the N–CO bond. This is easily seen from the ^{13}C-NMR spectra wherein many resonances are split into narrowly separated *doublets*. Rotation around the latter bonds must be slow with respect to the NMR time scale at room temperature.

Scheme 4

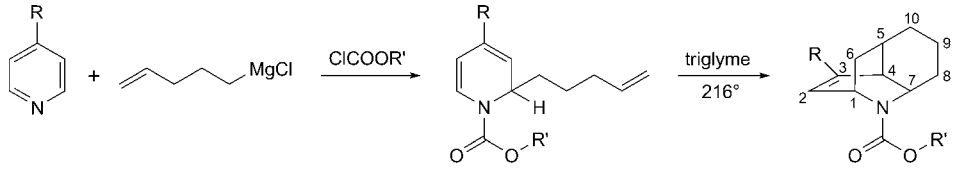

	R	R'
9a	^{t}Bu	Et
9b	Me	Me
9c	^{t}Bu	^{t}Bu

	R	R'
10a	^{t}Bu	Et
10b	Me	Me

Compounds **9a**, **9b**, and **9c** were heated under reflux in triethylene glycol dimethyl ether (triglyme) for 3 d at 216°. As shown in *Scheme 4*, the first two compounds underwent intramolecular *Diels–Alder* cyclizations to **10a** and **10b**, while **9c** aromatized to **11** (*Scheme 5*). In the case of **9c**, it is not unreasonable that aromatization would involve cycloelimination of isobutane. A preliminary proposal for a transition state for such a process would be characterized by polarization of the ^{t}Bu–O bond and thus developing partial carbocationic character of the ^{t}Bu moiety (see **12**‡). Such an elimination of alkane would be energetically favored for **9c** compared to **9a** and **9b**.

Scheme 5

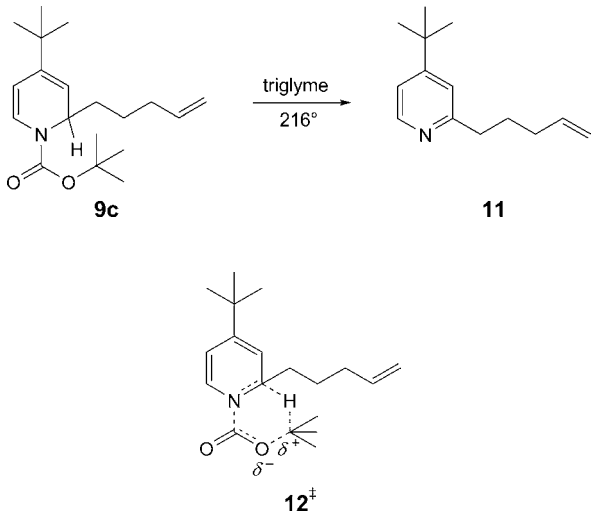

The NMR spectra for the crude products **10a** and **10b** indicated the presence of small amounts of solvent. Otherwise these spectra were identical to those for the products purified by chromatography, thus showing that the reactions were almost quantitative. However, in each case *ca.* 50% of the product became lost during chromatography, possibly due to complex chemical transformations induced by absorbent silica (SiO_2). Similar effects have been noted in the literature [3].

As **10a** and **10b** did not crystallize, it was decided to convert one to the corresponding amine. Compounds **10a** and **10b** were resistant to direct hydrolysis, including treatment with KOH in MeOH. However, treatment of **10a** with BuLi in hexane/Et_2O, followed by aqueous hydrolysis, gave a light yellow oil after workup, whose NMR spectra were consistent with the expected free amine **13** (see below). We were unable to produce a crystalline picrate from **13**. However, **13** reacted cleanly with 1-chloro-2,4-dinitrobenzene to give the easily crystallized *N*-(2,4-dinitrophenyl) derivative of **13** [5] (see **14**). The NMR data for **14** were consistent with the assumed *Diels–Alder* structure and were similar to those for **10a**, **10b**, and **13** as described below.

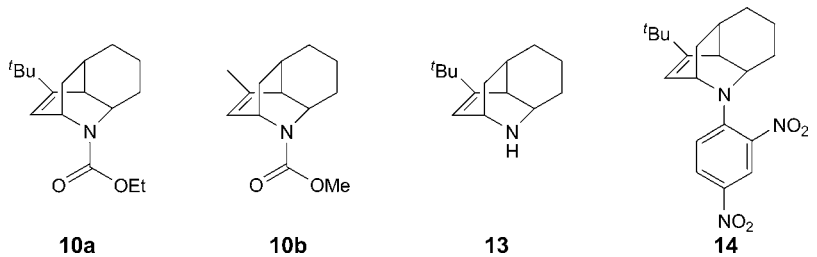

NMR. Not unexpectedly, the NMR data for **10a**, **10b**, **13**, and **14** were quite similar. The narrow equal *doublet*s of many of the resonances of **10a** and **10b** are most likely due to the presence of a 1:1 mixture of rotamers around the N–CO bond under conditions of slow rotation at room temperature with respect to the NMR time scale. The NMR data of **10a** in $CDCl_3$ are displayed in *Fig. 1* (^{1}H-NMR at 800.13 MHz), *Fig. 2* (^{13}C-APT; at 75.47 MHz), *Fig. 3* (^{1}H- and ^{13}C-HETCOR; at 800.13 and 201.2 MHz, resp.), and *Fig. 4* (^{1}H- and ^{13}C-INADEQUATE experiment; at 600.13 and 150.9 MHz, resp.). Initial assignments of NMR spectra were based on the method of synthesis, together with correlations of shifts and coupling patterns with published data of compounds with similar structural features to ours, *N*-(alkoxycarbonyl)-1,2-dihydropyridines (*Scheme 1*), and, for our *Diels–Alder* products, published NMR data for the *Diels–Alder* cyclization product **8** from 2-(but-3-en-1-yl)-4-(*tert*-butyl)-1-(ethoxycarbonyl)-1,2-dihydropyridine (**7**; Z = ^{t}Bu, $n = 2$; *Scheme 3*). The latter com-

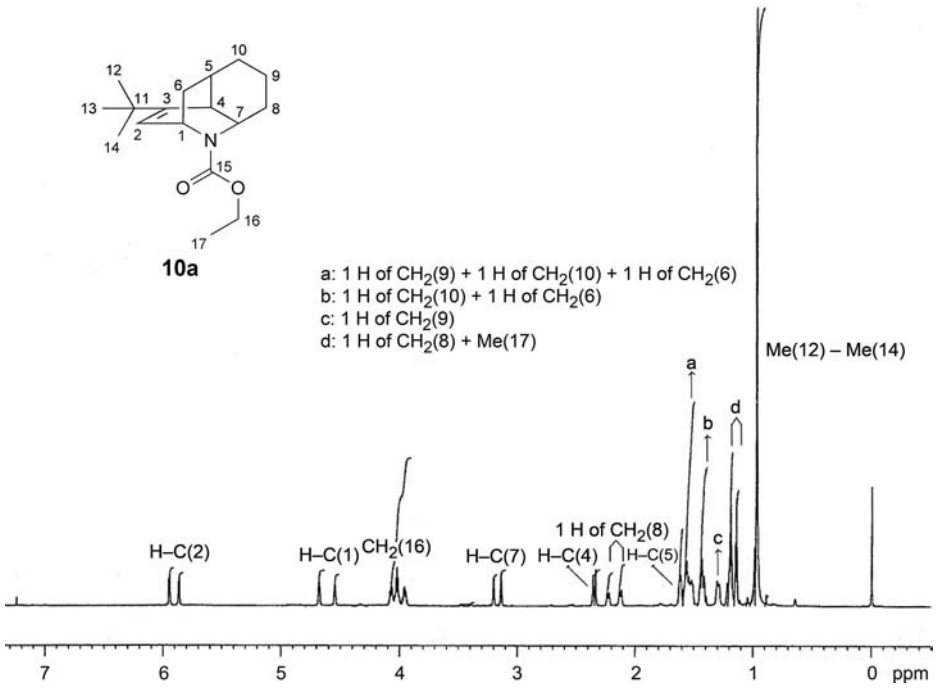

Fig. 1. *^{1}H-NMR Spectrum of* **10a** (at 800.13 MHz, in $CDCl_3$)

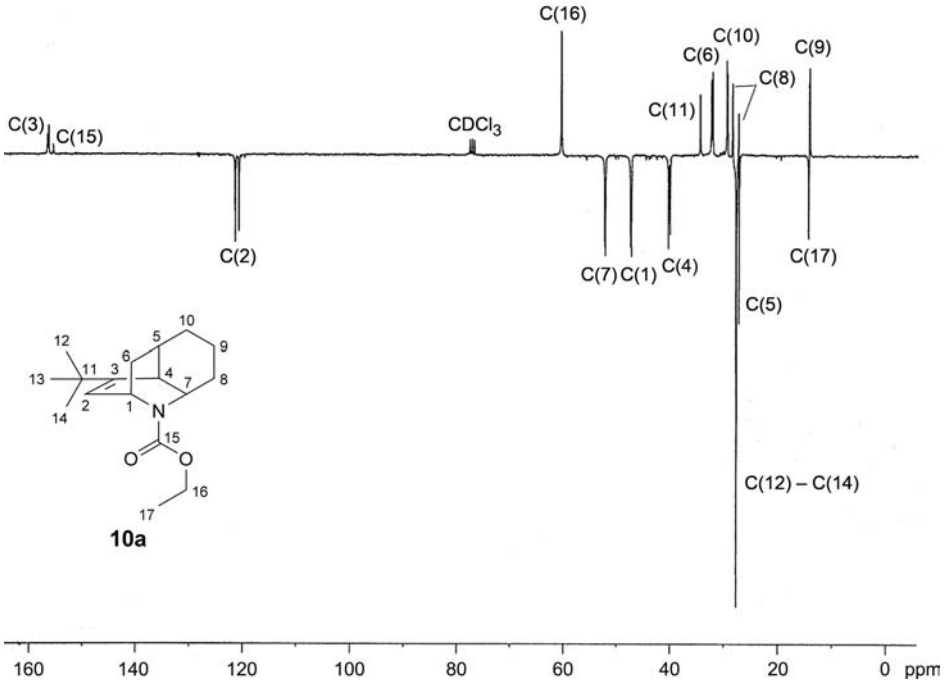

Fig. 2. *^{13}C-NMR Spectrum of* **10a** (APT; at 75.47 MHz, in $CDCl_3$)

pound shares the structural feature incorporated by C-atoms C(1), C(2), C(3), and C(7) in **10a** and **10b**. Further assignments were established by using the INADEQUATE experiment for **10a** displayed in *Fig. 4*, which was sufficient to assign the entire NMR data. Because of the low incidence of molecules at natural abundance with one pair of ^{13}C–^{13}C directly bonded, it was necessary to use a much higher concentrated solution (*ca.* 650 mg of **10a** in 0.5 ml of $CDCl_3$) than usual. Due to this concentration effect, the ^{13}C chemical shift values in the INADEQUATE plot are all *ca.* 1 ppm lower than in all our other NMR experiments. Also due to the very high concentration of **10a** used, the INADEQUATE data are not sufficiently resolved to reveal the narrow splitting due to rotamers. First, we assume that **10a** is indeed the intramolecular *Diels–Alder* product. Then, using the shift assignments made from previous correlations (*Fig. 3*) for C(1), C(2), C(3), and C(7), as δ(C) 47.5, 121, 156, and 52, respectively, we now list the correlations in the INADEQUATE plot as follows: from C(1) at 47.5 to 121 (C(2)) and 156 (C(3)), both given, and 32.4 which establishes C(6); from C(3) at 156 to 121 (C(2)), 34.5 (C_q(11)) and 40 (C(4)); from C(4) at 40 to 156 (C(3)), 27.3 (C(5)), and 52 (C(7)), the last two distinguished from electronegativity considerations; from C(5) at 27.3 to 40 (C(4)), 32 (C(6)), and 29.5 (C(10)), which establishes C(10); from C(10) at 29.5 to 27.3 (C(5)) and 14.4 (C(9)); from C(9) at 14.4 to 29.5 (C(10)) (the *doublet*s at 27.4 and 28.5 establish the C(8) shifts in both rotamers); and finally from C(11) at 34.5 to 156 (C(3)) and 27.8 (C(12)–C(14)). As noted, there is considerable overlap among the resonances of C(5), C(8), C(10), and C(12)–C(14), respectively.

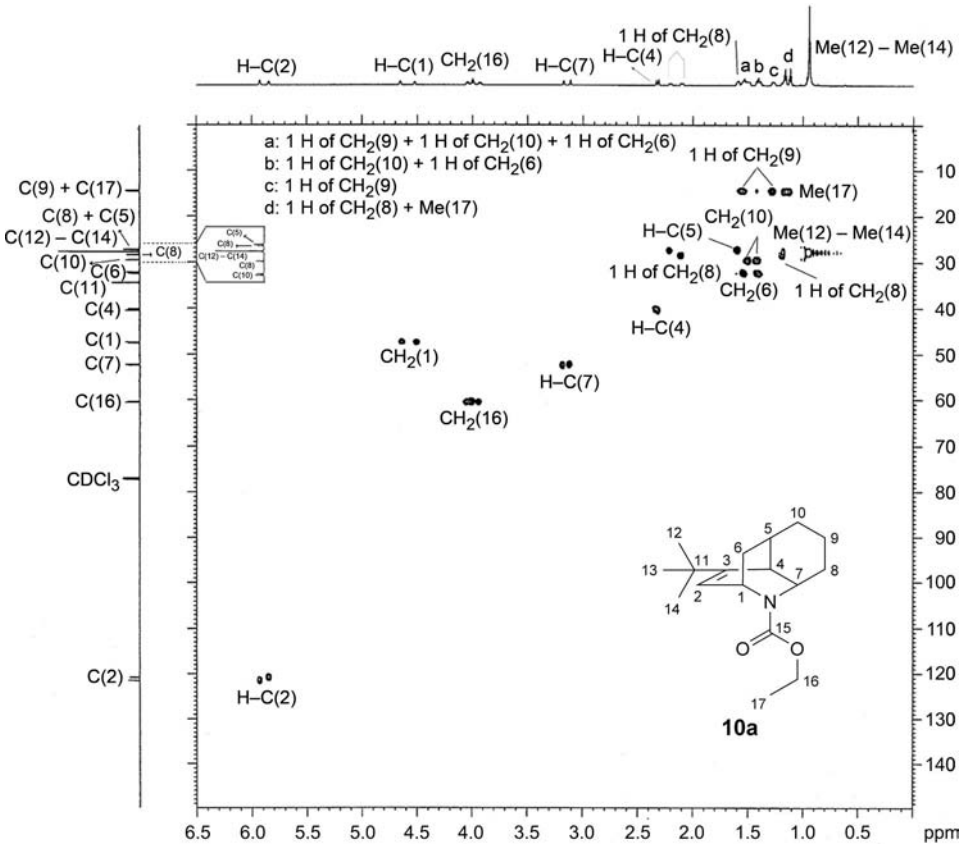

Fig. 3. *[1]H- and [13]C-NMR Spectra of* **10a** (HETCOR; at 800.13 and 201.21 MHz, resp., in $CDCl_3$)

However, C(5) and C(12) are distinguished in the APT plot (*Fig. 2*), since the Me C-atoms of the *t*Bu group (C(12) – C(14)) give the larger peak at δ(C) 27.8. Further, due to the proximity of one of the CH_2(8) H-atoms to the EtOCO O-atoms in each of the rotamers one would expect these H-atoms to show significant deshielding compared to all the other CH_2 hydrocarbon-like H-atom shifts. Thus the resonances on the HETCOR plot (*Fig. 3*) at δ(C) 28.5 and 27.4 must be assigned to C(8) in the two rotamers. The first C-atom signal correlates with directly bonded H-atoms signal at δ(H) 2.23 and 1.19, and the second with those at δ(H) 1.18 and 2.11. The H-atom shifts at δ(H) 2.1 and 2.23 are unusually deshielded for a non-polar hydrocarbon environment. Hence, they are assigned as close to the EtOCO O-atoms in each of the two rotamers. As noted in retrospect, the complete NMR assignments for **10a** have been obtained from the above NMR data and independently of literature correlations. All the other hydrocarbon-like H-atom signals lie in the normal hydrocarbon region. All these assignments are consistent with the 1D ^{1}H-NMR, ^{13}C-APT, and HETCOR plots. As indicated above, all assignments were also noted in the INADEQUATE and HETCOR plots.

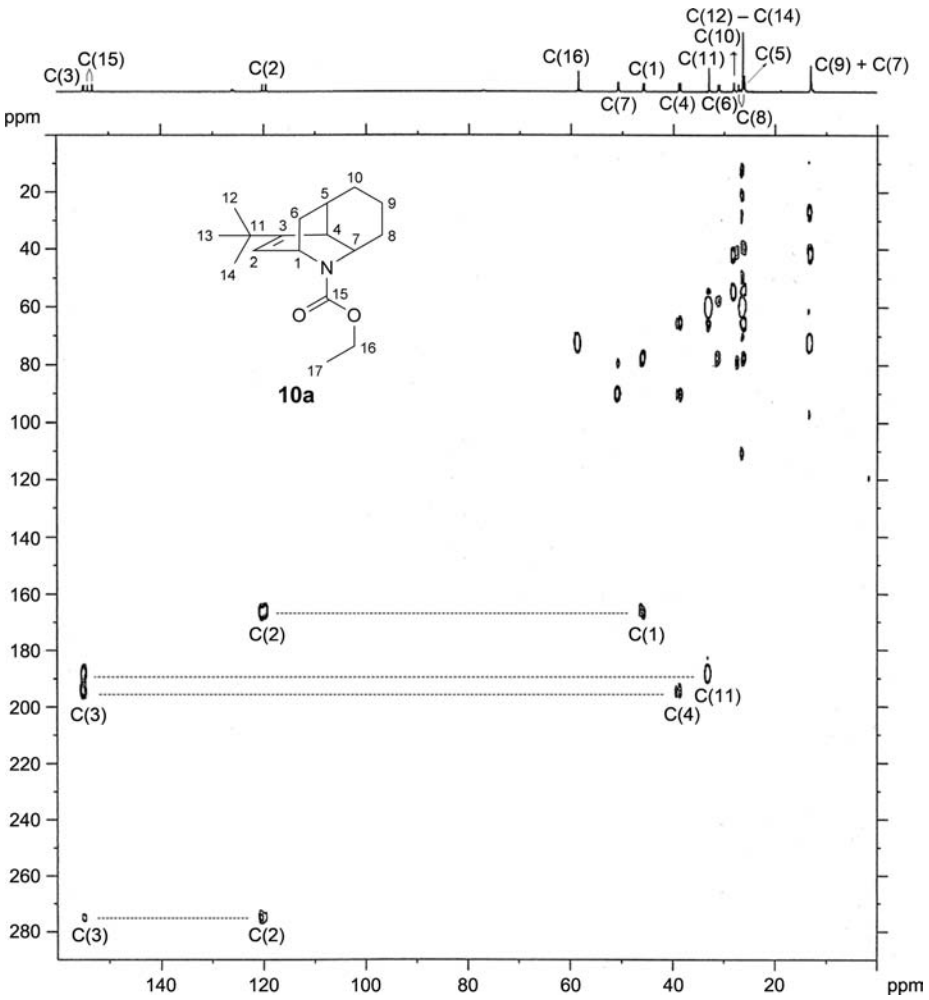

Fig. 4. *^{13}C-NMR Spectrum of* **10a** (INADEQUATE experiment; at 150.91 MHz, in $CDCl_3$)

Also, X-ray crystallography of **14** (see below) confirmed its assumed structure as well as, indirectly, the frameworks of **10a**, **10b**, and **13**. Finally, ^{13}C shifts of **14** calculated using DFT methods were very similar to the observed values (see below). Final chemical-shift assignments for **10a**, **10b**, **13**, and **14** are compiled in *Table 1*. *Fig. 5* compares calculated and observed ^{13}C shifts for **14**.

X-Ray Crystallography. Finally, the X-ray crystallographic results for **14** confirmed its *Diels–Alder* framework and, of course, those for **10a** and **13**, and by comparison to the NMR data of **10b**.

Compound **14** crystallizes with two molecules in the asymmetric unit labeled as **14A** and **14B**. There is an approximate twofold rotation axis (non-crystallographic symmetry) which relates the two molecules, and the axis lies approximately along

Table 1. *^{1}H- and ^{13}C-NMR Data of* **10a**, **10b**, **13**, *and* **14** (in $CDCl_3$; δ in ppm rel. to Me_4Si as internal standard, *J* in Hz). Labeling as in **10a** and **10b** with exception of the alkyl resonances of **10b**[a])[b]). The data in parentheses are of other rotomers of **10a** and **10b**.

Position	**10a**[c])		**10b**		**13**		**14**	
	δ(H)	δ(C)	δ(H)	δ(C)	δ(H)	δ(C)	δ(H)	δ(C)
1	4.66 (4.53)	47.5 (47.3)	4.48 (4.33)	46.9 (47.0)	3.31	47.1	3.91	56.2
2	5.92 (5.84)	121.4 (120.7)	5.76 (5.84)	125.0 (125.6)	5.79	122.0	5.84	120.1
3	–	156.3 (156.5)	–	143.9 (144.0)	–	155.5	–	157.7
4	2.32 (2.31)	40.3 (40.1)	2.22 (2.29)	44.2 (43.9)	2.07	38.8	2.61	40.3
5	1.60[d])	27.28 (27.26)	1.60[d])	25.8[d])	1.40	27.7	1.85	26.5
6	1.53 (1.41)	32.4 (32.1)	[e])	32.1 (31.9)	1.38/1.26	32.5	1.60/1.70	29.5
7	3.18 (3.12)	52.3 (52.2)	3.10 (3.15)	51.5 (51.4)	2.47	49.4	3.44	53.9
8	2.10 (2.21)	28.5 (27.4)	2.01 (1.02)	27.9 (26.9)	1.41/1.28	29.3	1.88	26.8
9	1.55 (1.28)	14.4 (14.3)	1.43 (1.14)	14.0 (15.0)	1.70/1.17	13.7	1.40	14.7
10	1.41 (1.53)	29.5 (29.4)	1.34 (1.22)	29.0 (28.9)	1.53/1.16	30.61	2.10/1.52	30.4
15	–	156.2 (155.3)	–	156.4 (155.4)	–	–	–	–
12–14	0.94[d])	27.8[d])	1.60[d])[a])	19.1[d])[a])	0.86	27.7	1.06	27.8
11	–	34.5[d])	–	–	–	34.1	–	34.8
17	1.12 (1.16)	14.4[d])	3.439[b]) (3.435[b]))	51.5[b]) (51.4[b]))	–	–	–	–
16	4.00	60.5 (60.4)	–	–	–	–	–	–

[a]) Me (at C(3)) in **10b**. [b]) MeO in **10b**. [c]) Recorded at 800 MHz. [d]) Single resonance only. [e]) Not resolved.

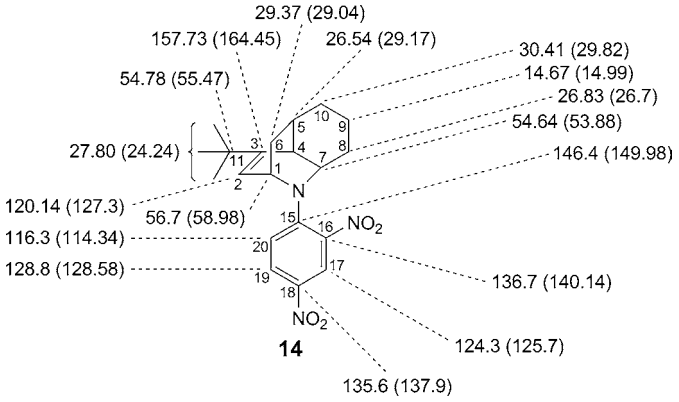

Fig. 5. *^{13}C-NMR Chemical shifts of* **14** *observed and* (calculated), δ, *using B3LYP/6-311G*, G1AO.* *, Means average.

the direction of the *c* axis of the unit cell. Due to the close proximity of **14A** and **14B**, within the *Van der Waals* radii, compared to neighboring molecules in the crystal, we shall describe the pair as a cluster and name it **14A** · **14B**, keeping in mind that the interaction between the components must be very small. The ORTEP diagram of **14A** · **14B** is shown in *Fig. 6*, and structural parameters of **14A** are collected in *Figs. 7* and *8*.

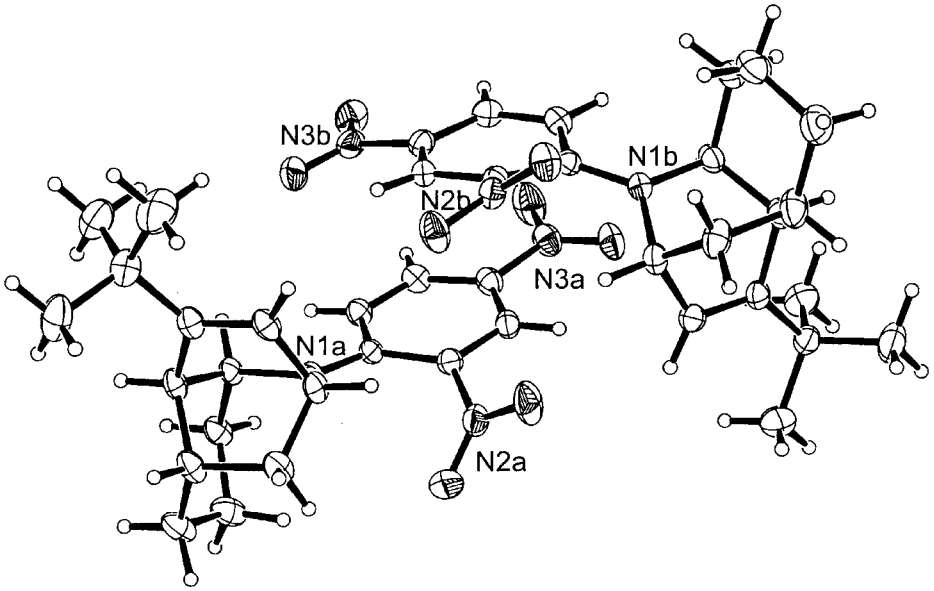

Fig. 6. *ORTEP Plot of the* **14A** · **14B** *cluster*

The NMR data for **14** in $CDCl_3$ solution are consistent for a single molecular species. The crystal structures of **14A** and **14B** only show one rotamer around the N(amine)–O(aromatic) bond. In both **14A** and **14B**, the *ortho*-NO_2 group lies on the opposite side of the molecule with respect to the ^{t}Bu group. This is also consistent with the NMR data.

The polycyclic frameworks of **14A** and **14B** each incorporate a typical chair cyclohexane for **14A**, *i.e.*, C(5A), C(4A), C(7A), C(8A), C(9A), and C(10A), and the same numbers for **14B**, as can easily be seen by inspection of the ORTEP plots above. Also the 'leaves' of the bicyclo[2.2.2]octene tryptic are all near planar as shown by the torsional angles **14A**, *i.e.*, C(1A), C(2A), C(3A), and C(4A), 1.3(3)°; C(1A), N(1A), C(7A), and C(4A), 2.0(2)°; C(4A), C(5A), C(6A), and C(1A), 2.4(3)°.

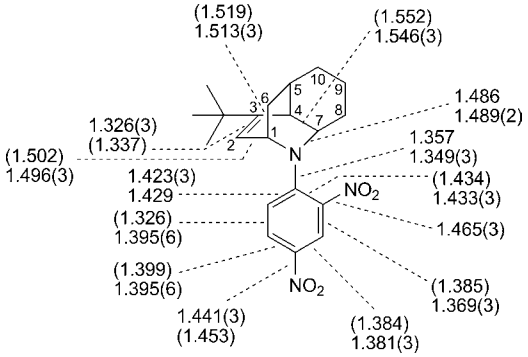

Fig. 7. *Selected X-ray crystallographic and* (calculated B3LYP/6-311G*) *bond lengths of* **14A** (in Å)

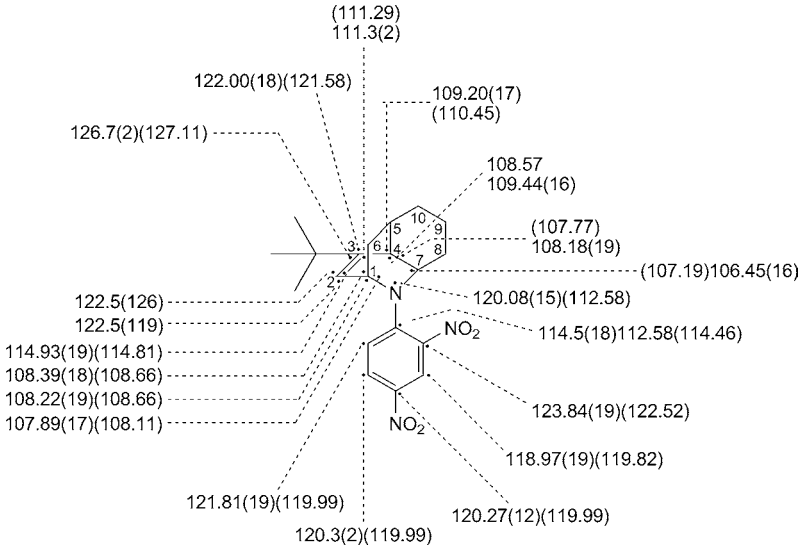

Fig. 8. *Selected X-ray crystallographic and* (calculated) *B3LYP/6-311G* bond angles* (in °) *of* **14A**

The aromatic rings of **14A** and **14B** are slightly distorted from planarity, as shown in *Table 2*, which lists the distances of different atoms of the (dinitrophenyl)amino moiety in **14A** with respect to the least-squares plane for the four aromatic C-atoms C(16A), C(17A), C(19A), and C(20A). Especially noticeable are the deviations of N–O bonds from coplanarity with the above least-squares plane. *Table 2* also lists the equivalent distances for **14B**. The resulting bow-shaped distortion of the aromatic rings is best conveyed by *Fig. 9*, which shows the side views of the aromatic parts of **14A** and **14B**. Note especially how the *ortho*-NO_2 groups are bent out of the aromatic planes. Similar effects have been reported from X-ray crystallographic studies of a variety of 2,4-dinitroanilines [6]. In fact, these aromatic distortions may well be due to steric repulsions between N–O O-atoms *ortho* to the amine N-atom.

Table 2. *Distances* ([Å]) *of Different Atoms in the Aromatic Moiety of* **14** *with Respect to the Least-Squares Plane Put through for Aromatic C-Atoms Indicated in the Table*

14A		**14B**		**14A**		**14B**	
C(16A)	0.013(1)[a])	C(16B)	0.014(1)[a])	N(2A)	0.331(4)	N(2B)	0.419(4)
C(17A)	−0.013(1)[a])	C(17B)	−0.014(1)[a])	N(3A)	−0.156(5)	N(3B)	−0.235(5)
C(19A)	0.013(1)[a])	C(19B)	0.014(1)[a])	O(1A)	1.194(5)	O(1B)	1.079(5)
C(20A)	−0.013(1)[a])	C(20B)	−0.014(1)[a])	O(2A)	−0.264(4)	O(2B)	0.151(4)
C(15A)	−0.118(3)	C(15B)	−0.167(3)	O(3A)	−0.242(6)	O(3B)	−0.362(6)
C(18A)	−0.048(3)	C(18B)	−0.074(3)	O(4A)	−0.195(6)	O(4B)	−0.283(6)
N(1A)	−0.366(5)	N(1B)	−0.505(5)				

[a]) Atom used to define the least-squares plane.

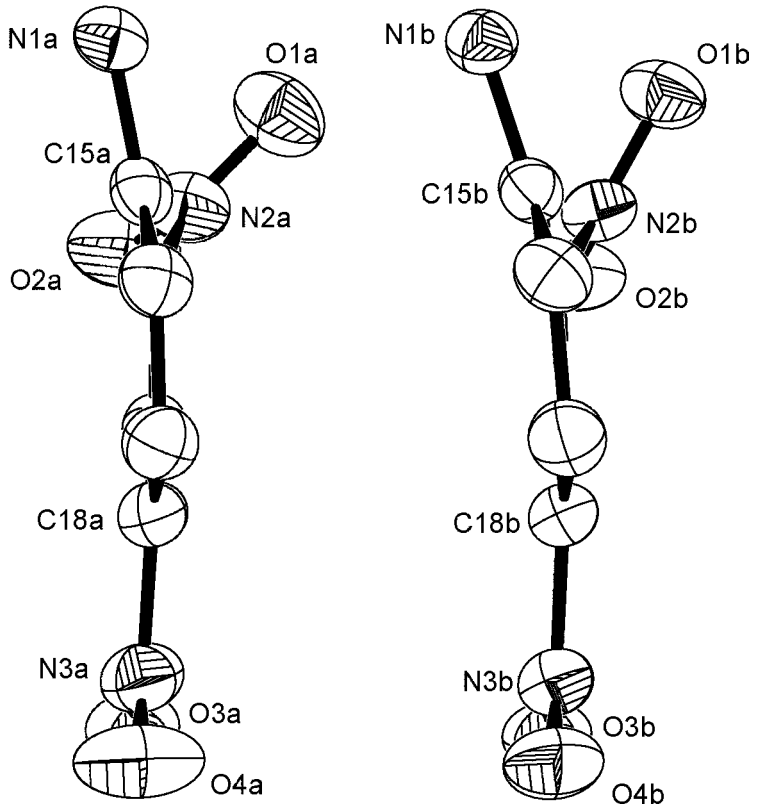

Fig. 9. *X-Ray crystallographic side view of aromatic rings of* **14A** *and* **14B** *within* **14A · 14B** *cluster*

The closest separations between **14A** and **14B** within the **14A · 14B** cluster are between sites on the slip-stacked aromatic rings, between, respectively, two C-atoms, C-atom, and O-atom, and between C-atom and N-atom (see *Table 3*). These separations are close to the sums of the respective *Van der Waals* radii (*Table 3*). Similar results

Table 3. *Closest Separations between* **14A** *and* **14B** *within the* **14A · 14B** *Cluster* ([Å])

Sites		X-Ray	WOW[a])	B3LYP 6-311G*	ωB97XD/6-311G*
C(18A)	C(19B)	3.338	3.46	3.585	3.317
C(19A)	N(3B)	3.221	3.25	3.682	3.325
C(19A)	O(4B)	3.190	3.22	3.567	3.496
C(20A)	N(3B)	3.205	3.25	3.567	3.317
C(20A)	O(3B)	3.163	3.22	3.602	3.295
O(2A)	C(2B)	3.153	3.22	3.540	3.318
O(3A)	C(20B)	3.287	3.22	3.602	3.295
N(3A)	C(19B)	3.394	3.25	3.567	3.352

[a]) Sum of *Van der Waals* radii, Table 12 in [7].

were reported from X-ray crystallographic studies of 1-(*cis*-2,6-dimethylpiperidine-1-yl)-2,4-dinitrobenzene [6g]. Such interactions have been ascribed to dispersion forces [8]. Note, however, that, whereas for the latter compound these interactions take place between neighboring molecules in zigzag slip-stack fashion throughout the crystal lattice [8] (*Fig. 10, a*), in the case of **14A**·**14B**, the close dispersion interactions are largely between **14A** and **14B** within the dimer (*Fig. 10, b*). This restriction is most likely due to the bulky substitution on the amine N-atom.

Computations[1]). We have constructed DFT models of **14** and of **14A**·**14B** cluster as entities in the gas phase or in non-polar solution using B3LYP/6-311G*, B3LYP/6-311 + G* [9][10], and ωB97XD/6-311G* [11]. Full geometry optimizations were carried out using these models, and frequency calculations served to confirm the stabilities of the calculated geometries. All these models closely reproduced the X-ray structure of the **14A**·**14B** cluster (see, *e.g.*, *Figs. 7* and *8*, which compare the X-ray crystallographic and B3LYP/6-3-11G* calculated structural parameters for **14A**). Further, the calculated structures for **14A** and **14B** in the cluster, and **14** are almost identical. In addition, using these results together with GIAO [12], the calculated ^{13}C-NMR shifts for **14**, and **14A** and **14B** are all closely similar to those observed for **14** in $CDCl_3$ solution (see *Fig. 5*), thus providing further support for DFT as a model for **14**. The major deviations between calculated and experimental ^{13}C-NMR chemical shifts of **14** were for the olefinic C-atoms C(2) and C(3), most likely due to interactions between the π structure of **14** with $CDCl_3$ solvent. In addition, this calculation clarified the ^{13}C-NMR shift assignments of C(8), C(9), and C(10) of **14** and by comparison with those C-atoms of **10a**, **10b**, and **13**.

However, in contrast to the agreement among the NMR results, B3LYP overestimated the smallest separations between **14A** and **14B** within the **14A**·**14B** cluster by 0.2 Å (see *Table 3*). Failure of B3LYP to account for dispersion interactions has already been noted [13]. Corrections proposed to account for dispersion effects [14] include ωB97XD/6-3-11G* [11]. As seen from *Table 3*, this procedure does more closely account for the smallest separations between **14A** and **14B** within the **14A**·**14B** cluster compared to the B3LYP calculations.

Finally, it may be suggested that, in case **14** is dimeric in solution, a calculation which makes use of the BSSE (Basic Set Superposition Error) [15] energy correction might be appropriate of the energy of interaction of **14A** and **14B** within the hypothetical dimeric cluster. Since we have no evidence that **14** is aggregated in $CDCl_3$ solution such a calculation is not now within the bounds of this study.

Conclusions. – An efficient route to a hetero polycyclic analog of the alkaloid framework, *via Diels–Alder* cyclization of a 1,2-dihydropyridine, has been firmly established using a combination of X-ray crystallography, calculations, and NMR. The structure of its 2,4-dinitrophenyl derivative shows interesting geometric distortions, as well as unusual dimeric clustering in the solid state.

---

[1]) Computational data are available from the authors.

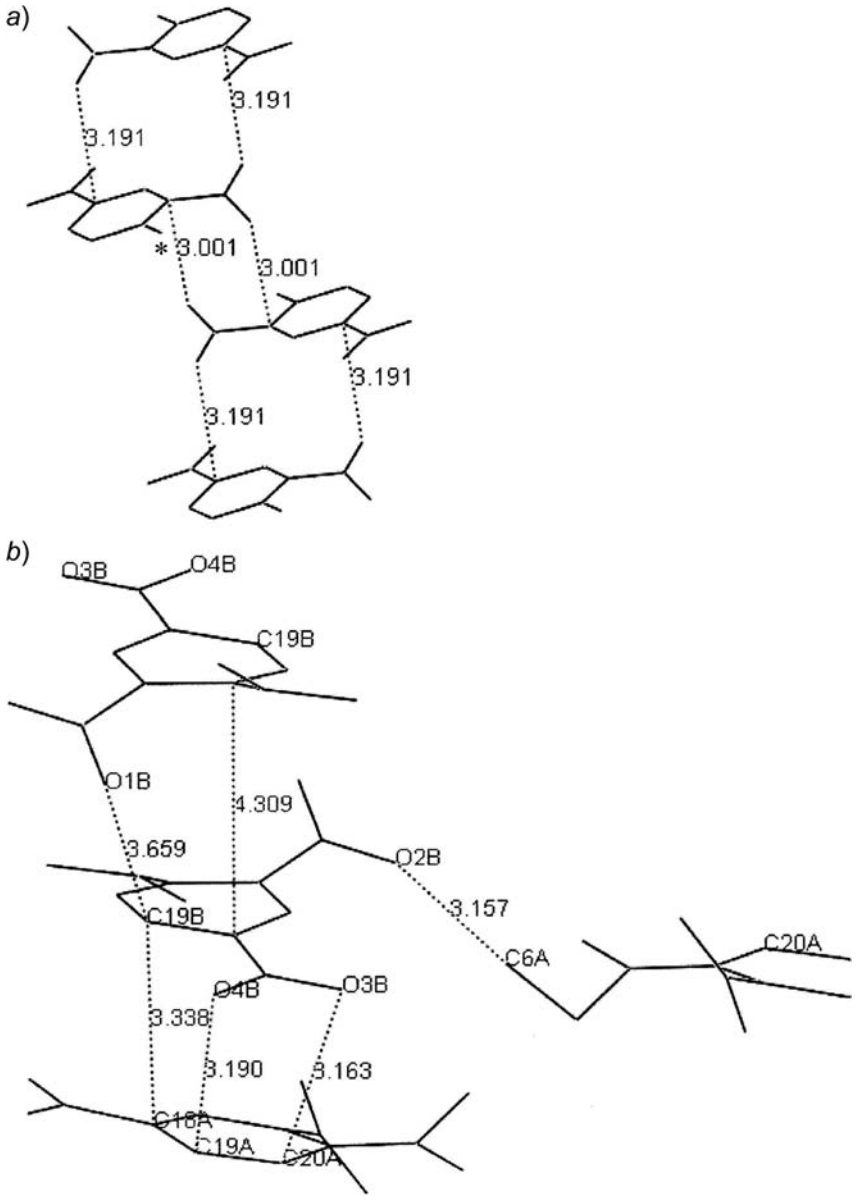

Fig. 10. a) *Intermolecular stacking in the solid state showing closest separations between molecules of 1-(*cis*-2,6-dimethylpiperidine-1-yl)-2,4-dinitrobenzene [*6g*]*. Amino substituent is abbreviated as a single bond, see *. b) *Closest separations* (in Å), *between* **14A** *and* **14B** *within the dimeric cluster* **14A**·**14B** *and further apart between clusters.* Both figures show the dinitrophenyl portion with abbreviated amino substituent.

This work was generously supported by grants from the *National Science Foundation* (Grant No. 1058035). We thank our Central Campus Instrumentation Center for technical assistance with the NMR equipment.

Experimental Part

General. Commercially available materials were used without purification. TLC: silica gel (SiO_2; *Silicycle*). Colum chromatography (CC): SiO_2 (*Silicycle*). ^{1}H- and ^{13}C-NMR spectra: *Bruker Avance 300*; δ in ppm rel. to Me_4Si as internal standard, J in Hz.[2]) HR-MS: *Waters QTOF*; in m/z.

*Ethyl 4-(*tert*-Butyl)-2-(pent-4-en-1-yl)pyridine-1(2*H*)-carboxylate* (**9a**). Under Ar at r.t., Mg turnings (3.4 g, 0.140 g atom) and dry THF (45 ml) were loaded into a flask equipped with a reflux condenser. Then, 5-bromopent-1-ene (16.6 ml, 20.9 g, 140 mmol) in 45 ml of dry THF was added dropwise, and the soln. was maintained at a gentle reflux for *ca.* 1.5 h. The mixture was allowed to stir for an additional h at r.t. After cannulating the resulting soln. into a second flask and cooling to 0°, 4-(*tert*-butyl)pyridine (10.34 ml, 9.46 g, 70 mmol) was added, and the mixture was stirred for 10 min, followed by dropwise addition of ClCOOEt (6.69 ml, 7.6 g, 70 mmol) over 10 min. The soln. was then stirred for another 1.5 h at 0°. Degassed H_2O (40 ml) was added to quench the reaction. The mixture was extracted with Et_2O (3 × 60 ml), and the org. phases were combined and dried ($MgSO_4$). Solvent was removed by rotary evaporation and then *in vacuo*, and the residues were separated by CC (SiO_2; AcOEt/hexane 1:19) to give **9a** (7.2 g, 37%). ^{1}H- and ^{13}C-NMR spectra indicated that the two conformers of dihydropyridine derivative **9a** were formed. ^{1}H-NMR (300 MHz, $CDCl_3$, 290 K): 6.71, 6.60 (2*d*, N–C*H*=CH, 0.40 H + 0.56 H); 5.85–5.62 (*m*, C*H*=CH_2); 5.36, 5.26 (2*d*, C*H*–*C*(^{t}Bu)–C*H*, 0.47 H + 1.58 H); 4.90 (*t*, =CH_2); 4.79–4.65, 4.65–4.55 (2*m*, N–CH, 0.6 H + 0.4 H); 4.16 (*q*, CH_2O); 1.97 (*q*, CH_2=CH–CH_2); 1.60–1.46, 1.46–1.30 (2*m*, CH_2–CH_2); 1.24 (*tt*, *Me*CH_2); 1.00 (*s*, ^{t}Bu) ^{13}C-NMR (75 MHz, $CDCl_3$, 290 K): 154.1, 153.2 (C=O); 142.2, 141.7 (*C*–^{t}Bu); 138.6, 138.5 (*C*H=CH_2); 125.0, 124.3 (N–*C*H=CH); 114.4, 114.3 (=CH_2); 113.9, 113.5 (CH=); 106.4, 105.9 (CH=); 61.8 (CH_2O); 52.0, 51.9 (N–CH); 33.6, 33.5, 33.4, 33.3, 33.1 (CH_2, Me_3C); 28.7 (*Me*$_3$C); 23.6, 23.5 (CH_2); 14.4 (*Me*CH_2O). HR-Q-TOF-MS: 300.1927 ([M + Na]$^+$, $C_{17}H_{27}NNaO_2^+$; calc. 300.1939).

*Methyl 4-Methyl-2-(pent-4-en-1-yl)pyridine-1(2*H*)-carboxylate* (**9b**). Under Ar at r.t., Mg turnings (2.21 g, 0.091 g atom) and dry THF (45 ml) were loaded into a flask equipped with a reflux condenser. Then, 5-bromopent-1-ene (10.9 ml, 13.7 g, 92 mmol) in 45 ml of dry THF was added dropwise, and the soln. was maintained at a gentle reflux for *ca.* 1.5 h. The mixture was allowed to stir for an additional h at r.t. After cannulating the resulting soln. into a second flask and cooling to 0°, 4-methylpyridine (4.4 ml, 4.21 g, 45 mmol) was added, and the mixture was stirred for 10 min, followed by dropwise addition of ClCOOMe (3.17 ml, 3.87 g, 41 mmol) over 10 min. The soln. was stirred for another 1.5 h at 0°. Degassed H_2O (5.4 ml) was added to quench the reaction, and the precipitate was removed by filtration. The filtrate was dried ($MgSO_4$). Solvent was removed by rotary evaporation and then *in vacuo*, and the residues were separated by CC (SiO_2; AcOEt/hexane 1:19) to afford **9b** (4.8 g, 52.5%). ^{1}H-NMR (300 MHz, $CDCl_3$, 290 K): 6.62, 6.47 (2*d*, N–C*H*=CH); 5.80–5.50 (*m*, CH_2C*H*=CH_2); 5.22–5.08 (br., C*H*–*C*(^{t}Bu)); 5.04, 4.96 (2*d*, C*H*–*C*(^{t}Bu)); 4.82 (*t*, =CH_2); 4.69–4.51, 4.51–4.38 (2*m*, N–CH); 3.65 (*s*, MeO); 1.90 (*q*, CH_2=CH–CH_2); 1.62 (*s*, Me); 1.58–1.40, 1.40–1.19 (2*m*, CH_2–CH_2, 1.35 H + 3.31 H). ^{13}C-NMR (75 MHz, $CDCl_3$, 290 K): 154.4, 153.5 (C=O); 138.3 (*C*H=CH_2); 129.4, 128.8 (*C*–Me); 124.7, 123.9 (N–*C*H=CH); 117.5, 116.9 (CH=); 114.2 (=CH_2); 109.1, 108.8 (CH=); 52.6, 52.0 (N–CH, MeO); 33.6, 33.4, 33.2, 33.8 (CH_2); 23.4, 23.2 (CH_2); 20.1. HR-Q-TOF-MS: 162.14 ([M – COOMe]$^+$, $C_{11}H_{16}N^+$; calc. 162.13).

tert-*Butyl 4-(*tert*-Butyl)-2-(pent-4-en-1-yl)pyridine-1(2*H*)-carboxylate* (**9c**). A mixture of redistilled ^{t}BuOH (6.7 ml, 5.19 g, 70 mmol), dry 4-(*tert*-butyl)pyridine (20.68 ml, 18.92 g, 140 mmol), and dry THF (200 ml) was cooled to −78° under Ar. Then, a 20% $COCl_2$ soln. (37 ml, 70 mmol) in toluene was added dropwise within 30 min. A large amount of 4-(*tert*-butyl)pyridinium chloride precipitated, and vigorous

---

[2]) The ^{1}H- and ^{13}C-NMR spectra of new compounds are available as *Supplementary Material* from the corresponding author.

stirring was continued for 1 h. The mixture was warmed to 0°. Then, the *Grignard* reagent prepared as described above from 5-bromopent-1-ene (10.4 g, 70 mmol) in THF (100 ml) was added slowly over 30 min, and stirring was continued for another 30 min. The reaction was quenched with degassed H_2O (40 ml), the resulting mixture was extracted with Et_2O (3×60 ml), and the org. phases were combined and dried ($MgSO_4$). Solvent was removed by rotary evaporation and *in vacuo*. Finally, the residues were separated by CC (SiO_2; AcOEt/hexane 1:19) to yield **9c** (2 g, 9.4%). ^{1}H-NMR (300 MHz, $CDCl_3$, 290 K): 6.68, 6.53 (2*d*, N–C*H*=CH); 5.81–5.60 (*m*, CH_2–C*H*=CH_2); 5.20 (br., C*H*–C(*t*Bu)); 4.87 (*t*, =CH_2); 4.72–4.59, 4.59–4.40 (2*m*, N–CH); 1.94 (*q*, CH_2=CH–CH_2); 1.42 (*s*, $COOCMe_3$); 1.40–1.22 (*m*, CH_2–CH_2); 0.98 (C–CMe_3). ^{13}C-NMR (75 MHz, $CDCl_3$, 290 K): 152.9, 152.0 (C=O); 142.2, 141.7 (*C*–CMe_3); 138.5, 138.4 (*C*H=CH_2); 124.9 (N–*C*H=CH); 114.4, 114.2 (=CH_2); 113.6, 113.3 (CH=); 105.6, 105.0 (CH=); 80.5 (Me_3CO); 52.2, 51.2 (N–CH); 33.6, 33.3 (CH_2, C–*C*Me_3); 28.7, 28.1 (*Me*$_3$C); 23.6 (CH_2). HR-Q-TOF-MS: 328.2249 ($[M+Na]^+$, $C_{19}H_{31}NNaO_2^+$; calc. 328.2252).

Ethyl 8-(tert-Butyl)-1,2,3,4,4a,5,6,8a-octahydro-1,6-epiminonaphthalene-9-carboxylate (**10a**). Under Ar, **9a** (7.2 g, 26 mmol) was refluxed in triglyme (72 g) at 216° for 3 d. The solvent was removed by distillation under reduced pressure. The NMR spectra and TLC of the residue indicated almost quant. conversion to the intramolecular *Diels–Alder* adduct. Further purification by CC (SiO_2; AcOEt/hexane 1:3) gave **10a** (2.4 g, 33%) based on (**9a**). ^{1}H-NMR (300 MHz, $CDCl_3$, 290 K): 5.89, 5.85 (*dd*, H–C(2)); 4.63, 4.49 (*tt*, H–C(1)); 4.10–3.80 (*m*, $COOCH_2$); 3.14, 3.08 (2*s*, H–C(7)); 2.29 (*m*, H–C(4)); 2.12 (*dd*, 1 H of CH_2(8)); 1.65–1.30 (*m*, CH_2(10), CH_2(6), H–C(5), 1 H of CH_2(9)); 1.30–1.15 (*m*, 1 H of CH_2(9)); 1.15–1.02 (*m*, 1 H of CH_2(8), $COOCH_2$*Me*); 0.91 (*s*, *t*Bu). ^{13}C-NMR (75 MHz, $CDCl_3$, 290 K): 156.3, 156.1, 155.2 (C(3), C=O); 121.4, 120.7 (C(2)); 60.3 (CH_2O); 52.2, 52.1 (C(7)); 47.4, 47.2 (C(1)); 40.3, 40.0 (C(4)); 34.4 (Me_3C); 32.3, 32.0 (C(6)); 29.4, 29.3 (C(10)); 28.4, 27.2 (C(8)); 27.3 (*Me*$_3$C); 26.6 (C(5)); 14.4 ($COOCH_2$*Me*); 14.3, 14.2 (C(9)). ^{1}H-NMR (800 MHz, $CDCl_3$, 290 K): 5.92, 5.84 (*dd*, H–C(2)); 4.66, 4.53 (*tt*, H–C(1)); 4.11–3.90 (*m*, $COOCH_2$); 3.18, 3.12 (2*s*, H–C(7)); 2.32, 2.31 (2*s*, H–C(4)); 2.21, 2.10 (2*d*, 1 H of CH_2(8)); 1.60 (*d*, H–C(5)); 1.59–1.43 (*m*, 1 H of CH_2(9), 1 H of CH_2(10), 1 H of CH_2(6)); 1.41 (*t*, 1 H of CH_2(10), 1 H of CH_2(6)); 1.27 (*d*, 1 H of CH_2(9)); 1.16, 1.12 (2*t*, 1 H of CH_2(8), $COOCH_2$*Me*); 0.94 (*s*, Me_3C). ^{13}C-NMR (201 MHz, $CDCl_3$, 290 K): 156.5, 156.3 (C(3)); 156.2, 155.3 (C=O); 121.4, 120.7 (C(2)); 60.5, 60.4 (CH_2O); 52.3, 52.2 (C(7)); 47.5, 47.3 (C(1)); 40.4, 40.1 (C(4)); 34.5 (Me_3C); 32.4, 32.1 (C(6)); 29.5, 29.4 (C(10)); 28.5, 27.4 (C(8)); 27.8 (*Me*$_3$C); 27.3, 27.3 (C(5)); 14.5, 14.4, 14.4, 14.3 ($COOCH_2$*Me*, C(9)). HR-Q-TOF-MS: 300.1921 ($[M+Na]^+$, $C_{17}H_{27}NNaO_2^+$; calc. 300.1939).

Methyl 8-methyl-1,2,3,4,4a,5,6,8a-octahydro-1,6-epiminonaphthalene-9-carboxylate (**10b**). Under Ar, **9b** (2.4 g, 10.9 mmol) was refluxed in 15 g of triglyme at 216° over 2 d. The solvent was removed under reduced pressure. The NMR spectra of the crude product indicated almost quant. conversion to the *Diels–Alder* product contaminated with triglyme. Purification using CC (SiO_2; AcOEt/hexane 1:3) gave of **10b** (0.4 g, 16.7% based on **9b**). ^{1}H-NMR (300 MHz, $CDCl_3$, 290 K): 5.84, 5.76 (*dd*, H–C(2)); 4.60–4.40, 4.40–4.20 (*m*, H–C(1)); 3.44, 3.43 (2*s*, COOMe); 3.15, 3.10 (2*s*, H–C(7)); 2.15–1.85 (*m*, 1 H of CH_2(8), H–C(4)); 1.60 (*s*, Me–C(3)); 1.56 (*s*, H–C(5)); 1.50–1.34, 1.34–1.20 (2*m*, CH_2(10), CH_2(6), 1 H of CH_2(9)); 1.14 (*m*, 1 H of CH_2(9)); 1.10–0.90 (*m*, 1 H of CH_2(8)). ^{13}C-NMR (75 MHz, $CDCl_3$, 290 K): 156.4, 155.4 (C=O); 144.0, 143.9 (C(3)); 125.6, 125.0 (C(2)); 51.5, 51.4 (MeO); 51.1, 50.8 (C(7)); 47.0, 46.9 (C(1)); 44.2, 43.9 (C(4)); 32.1, 31.9 (C(6)); 29.0, 28.9 (C(10)); 27.9, 26.9 (C(8)); 25.8 (C(5)); 19.1 (*Me*–C(3)); 14.0, 15.0 (C(9)). HR-Q-TOF-MS: 244.1317 ($[M+Na]^+$, $C_{13}H_{19}NNaO_2^+$; calc. 244.1313).

4-(tert-*Butyl*)-*2-(pent-4-en-1-yl)pyridine* (**11**). Compound **9c** (2 g, 6.6 mmol) was refluxed in 20 g of triglyme at 216° for 1 d. Solvents and volatile materials were removed under distillation under reduced pressure. The NMR data of the crude product indicated almost quant. conversion to **11**. A pure sample, 0.1 g, was obtained by CC (SiO_2; AcOEt). ^{1}H-NMR (300 MHz, $CDCl_3$, 290 K): 8.30 (*d*, H–C(6)); 7.00 (*s*, H–C(3)); 6.95 (*d*, H–C(5)); 5.85–5.60 (*m*, C*H*=CH_2); 4.87 (*t*, =CH_2); 2.67 (*t*, N–C–CH_2); 2.01 (*q*, =CH–CH_2); 1.73 (*quint.*, N–C–CH_2–CH_2); 1.17 (*s*, *t*Bu). ^{13}C-NMR (75 MHz, $CDCl_3$, 290 K): 161.5, 159.8 (C(2), C(4)); 148.9 (C(6)); 138.2 (=CH); 119.4, 117.8 (C(3), C(5)); 114.6 (=CH_2); 37.7 (N–C–*C*H_2); 34.3 (Me_3C); 33.2 (=CH–CH_2); 30.3 (*Me*$_3$C); 28.9 (N–C–CH_2–*C*H_2). HR-Q-TOF-MS: 204.1755 ($[M+H]^+$, $C_{14}H_{22}N^+$; calc. 204.1752).

8-(tert-*Butyl*)-*1,2,3,4,4a,5,6,8a-octahydro-1,6-epiminonaphthalene* (**13**). Under Ar at −20 to −30°, BuLi (12 ml; 1.6M, 19.2 mmol, 3.9 equiv.) in hexane was added dropwise to **10a** (1.35 g, 4.87 mmol) in

20 ml of Et_2O. The mixture was allowed to warm to r.t. overnight with stirring. The reaction was quenched with MeOH (5 ml) and then H_2O (5 ml). The resulting soln. was acidified with 4 ml of aq. 37% HCl. The aq. phase was separated and neutralized to pH of *ca.* 10 with Na_2CO_3 soln., and the latter was extracted with CH_2Cl_2 (3×15 ml). The combined org. phase was dried ($MgSO_4$), and solvent was removed by rotary evaporation and *in vacuo* to afford 0.4 g of a light yellow oil whose NMR data were expected for **13**. ^{1}H-NMR (300 MHz, $CDCl_3$, 290 K): 5.79 (*d*, H–C(2)); 3.40–3.20 (*m*, H–C(1)); 2.47 (*s*, H–C(7)); 2.07 (*s*, H–C(4)); 1.99 (br., NH); 1.84–1.60 (*m*, 1 H of CH_2(9)); 1.60–1.46 (*m*, 1 H of CH_2 at δ(C) 30.6), 1.46–1.33 (*m*, 1 H of CH_2(6), 1 H of CH_2 at δ(C) 29.3, H–C(5)); 1.33–1.08 (*m*, 1 H of CH_2(6), 1 H of CH_2 at δ(C) 30.6, 1 H of CH_2 at δ(C) 29.3, 1 H of CH_2(9)); 0.86 (*s*, ^{t}Bu). ^{13}C-NMR (75 MHz, $CDCl_3$, 290 K): 155.5 (C(3)); 122.0 (C(2)); 49.4 (C(7)); 47.1 (C(1)); 38.8 (C(4)); 34.1 (Me_3C); 32.5 (C(6)); 30.6 (CH_2); 29.3 (CH_2); 27.7 (Me_3C, C(5)); 13.7 (C(9)).

8-(tert-*Butyl*)*-1,2,3,4,4a,5,6,8a-octahydro-9-(2,4-dinitrophenyl)-1,6-epiminonaphthalene* (**14**). A sample of **13** (0.27 g, 1.4 mmol), mixed with 2,4-dinitrochlorobenzene (0.278 g, 1.4 mmol) and K_2CO_3 (0.2 g, 1.4 mmol), was refluxed in 3 ml of MeOH for 1 h as described in [5], cooled to r.t., and filtered to afford 0.48 g of yellow powder. NMR data indicated almost quant. conversion of **13** to **14**. ^{1}H-NMR (300 MHz, $CDCl_3$, 290 K): 8.63 (*d*, 1 arom. H); 8.10 (*dd*, 1 arom. H); 6.82 (*d*, 1 arom. H); 5.84 (*dd*, H–C(2)); 3.99–3.82 (*m*, H–C(1)); 3.44 (*s*, CH(7)); 2.61 (*d*, H–C(4)); 2.10 (*dt*, 1 H of CH_2(6)); 2.00–1.75

Table 4. *Crystallographic Data of* **14** *and Structure-Refinement Details*

Formula	$C_{20}H_{25}N_3O_4$
M_r	371.43
Crystal size [mm]	$0.15 \times 0.15 \times 0.31$
Temp. [K]	210(2)
Radiation type	MoK_α (0.71073 Å)
Crystal system	triclinic
Space group	$P\bar{1}$
Z	4
Unit cell dimensions:	
a [Å]	11.4885(2)
b [Å]	12.6257(2)
c [Å]	14.7269(2)
α [°]	65.327(1)
β [°]	81.496(1)
γ [°]	84.185(1)
V [Å^3]	1917.92(5)
D_x (calc.) [g cm^{-3}]	1.286
Absorption coefficient [mm^{-1}]	0.091
F(000)	792
θ Range for data collection	2.22–24.95°
Index ranges	$-13 \le h \le 13$, $-14 \le k \le 14$, $-17 \le l \le 17$
Reflections collected	47303
Independent reflections	6710 [$R_{int} = 0.044$]
Observed reflections [$I > 2\sigma(I)$]	4861
Completeness to $\theta = 24.95°$ [%]	99.6
Refinement method	Full-matrix least-squares on F^2
Data/restraints/parameters	6710/0/493
Goodness-of-fit on F^2	1.020
Final R indices [$I > 2\sigma(I)$]	$R^1 = 0.0539$, $wR^2 = 0.1390$
R Indices (all data)	$R^1 = 0.0795$, $wR^2 = 0.1541$
Largest diff. peak and hole [e Å^{-3}]	0.697; −0.307

(*dd*, 1 H of CH_2 at δ(C) 26.8, CH at δ(C) 26.5); 1.76 – 1.64 (*m*, 1 H of CH_2(10), 1 H of CH_2(9)); 1.61 – 1.44 (*m*, 1 H of CH_2(6), 1 H of CH_2(10)); 1.44 – 1.30 (*m*, 1 H of CH_2 at δ(C) 26.8, 1 H of CH_2(9)); 1.05 (*s*, ^{t}Bu). ^{13}C-NMR (75 MHz, $CDCl_3$, 290 K): 157.7; 146.4; 136.7; 135.6; 127.9; 124.3; 120.1; 116.1; 56.2 (C(7)); 53.9 (C(1)); 40.3 (C(4)); 34.8 (Me_3C); 30.4 (C(6)); 29.5 (C(10)); 27.8 (Me_3C); 26.8; 26.5; 14.7 (C(9)). Further crystallization from MeOH provided crystals suitable for X-ray crystallography. HR-Q-TOF-MS: 394.1752 ($[M+Na]^+$, $C_{20}H_{25}N_3NaO_4^+$; calc. 394.1743).

Crystallography[3]). Crystal data of **14** and parameters of refinement are compiled in *Table 4*. The data-collection crystal was a pale orange rectangular block. Data was collected on a *Nonius Kappa* CCD diffractometer at 210 K equipped with an *Oxford Cryosystems* cryostream cooler. The data-collection strategy was set up to measure a hemisphere of reciprocal space with a redundancy factor of 3.5, which means that 90% of these reflections were measured at least 3.5 times. Phi and omega scans with a frame width of 1.0° were used. Data integration was done with DENZO [16], and scaling and merging of the data was conducted with SCALEPACK [16].

The structure was solved in space group $P\bar{1}$ by direct methods according to SHELXS-97 [17]. There are two molecules in the asymmetric unit, labeled as **A** and **B**. Full-matrix least-squares refinements based on F^2 were performed in SHELXL-97 [17]), as incorporated in the WinGX package [18]).

For each Me group, the H-atoms were added at calculated positions using a riding model with $U(H) = 1.5 \cdot U_{eq}$(bonded C-atom). The torsion angle, which defines the orientation of the Me group about the C–C bond, was refined. The rest of the H-atoms was included in the model at calculated positions using a riding model with $U(H) = 1.2 \cdot U_{eq}$(bonded atom). Neutral atom scattering factors were used and include terms for anomalous dispersion [19].

REFERENCES

[1] a) G. Fraenkel, J. W. Cooper, C. M. Fink, *Angew. Chem., Int. Ed.* **1970**, *9*, 523; b) R. E. Lyle, J. L. Marshall, D. L. Comins, *Tetrahedron Lett.* **1977**, *18*, 1015; c) R. Yamaguchi, Y. Nakazona, M. Kawanisi, *Tetrahedron Lett.* **1983**, *24*, 1801.

[2] G. Fraenkel, J. W. Cooper, *J. Am. Chem. Soc*. **1977**, *93*, 7228.

[3] See for example: G. R. Krow, Y. B. Lee, S. W. Szczepanski, R. Raghavachari, *Tetrahedron Lett.* **1985**, *26*, 2617; G. R. Krow, Y. B. Lee, R. Raghavachari, S. W. Szczepanski, P. V. Alston, *Tetrahedron* **1991**, *47*, 8499.

[4] G. Fraenkel, J. W. Cooper, *Tetrahedron Lett.* **1968**, *9*, 1825.

[5] B. S. Furniss, A. J. Hannaford, P. W. G. Smith, A. R. Tatchell, 'Vogel's Textbook of Practical Organic Chemistry', 5th edn., Longman, New York, 1989, p. 1276.

[6] a) J. Ellena, G. Punte, B. E. Rivero, M. V. Remedi, E. B. de Vargas, R. H. de Rossi, *J. Chem. Crystallogr.* **1995**, *25*, 801; b) G. Punte, B. E. Rivero, S. E. Sukolovsky, N. S. Nudelman, *Acta Crystallogr., Sect. C* **1991**, *47*, 1222; c) G. Punte, B. E. Rivero, S. E. Sukolovsky, N. S. Nudelman, *Acta Crystallogr., Sect. C* **1989**, *45*, 1952; d) J. N. Low, M. S. V. Doidge-Harrison, J. Cobo, *Acta Crystallogr., Sect. C* **1996**, *52*, 964; e) L. Prasad, E. J. Gabe, Y. Le Page, *Acta Crystallogr., Sect. B* **1982**, *38*, 2780; f) G. Punte, B. E. Rivero, *Acta Crystallogr., Sect. C* **1991**, *47*, 2118; g) M. F. Mackay, D. J. Gale, J. F. K. Wilshire, *Aust. J. Chem.* **2000**, *53*, 715.

[7] M. Mantina, A. C. Chamberlin, R. Valero, C. J. Cramer, *J. Phys. Chem.* **2009**, *113*, 5806.

[8] R. Taylor, G. Kennard, *J. Am. Chem. Soc.* **1982**, *104*, 5063; G. R. Desiraju, *Acc. Chem. Res.* **1991**, *24*, 290; T. W. Panunto, Z. Urbanczyk-Lipowska, R. Johnson, M. G. Etter, *J. Am. Chem. Soc.* **1987**, *109*, 7786.

[9] A. D. Becke, *J. Chem. Phys.* **1993**, *98*, 5648; C. Lee, W. Yang, R. G. Parr, *Phys. Rev. B* **1988**, *37*, 785; S. H. Voska, L. Wilk, M. Nusair, *Can. J. Phys.* **1980**, *58*, 1200; P. J. Stephens, F. J. Devlin, C. F. Chabalowski, M. J. Frisch, *J. Phys. Chem.* **1994**, *98*, 11623.

---

[3]) CCDC-951426 contains the supplementary crystallographic data for this article. These data can be obtained free of charge *via* http://www.dc.ac.uk/data_requested/cif.

[10] A. D. McLean, G. S. Chandler, *J. Chem. Phys.* **1980**, *72*, 5639; K. Raghavachari, J. S. Binkley, R. Seeger, J. A. Pole, *J. Chem. Phys.* **1980**, *72*, 650.
[11] J.-D. Chai, M. Head-Gordon, *J. Chem. Phys.* **2008**, *128*, 84106; J.-D. Chai, M. Head-Gordon, *Phys. Chem. Chem. Phys.* **2008**, *10*, 6615.
[12] F. London, *J. Phys. Radium* **1937**, *8*, 394; R. McWeeny, *Phys. Rev.* **1962**, *126*, 1028; R. Ditchfield, *Mol. Phys.* **1974**, *27*, 789; K. Wolinsky, J. K. Hilton, P. Pulay, *J. Am. Chem. Soc.* **1990**, *112*, 8251; J. R. Cheeseman, J. W. Trucks, M. J. Frisch, *J. Chem. Phys.* **1996**, *104*, 5497.
[13] M. J. Allen, D. J. Tozer, *J. Chem. Phys.* **2002**, *117*, 11113.
[14] I.-C. Lin, A. Lilienfeld, M. D. Coutinho-Neto, I. Tavernelli, U. Rothlisbeger, *J. Phys. Chem. B* **2007**, *111*, 14346.
[15] R. Fletcher, *Mol. Phys.* **1970**, *19*, 55; S. Simon, M. Duran, J. J. Dannenberg, *J. Chem. Phys.* **1996**, *105*, 11024.
[16] Z. Otwinowski, W. Minor, *Methods Enzymol.* **1997**, *276*, 307.
[17] G. M. Sheldrick, SHELXS-97 and SHELXL-97, *Acta Crystallogr., Sect. A* **2008**, *64*, 112.
[18] L. J. Farrugia, WinGX-Version 1.70.01, *J. Appl. Crystallogr.* **1999**, *32*, 837.
[19] 'International Tables for Crystallography', Kluwer Academic Publishers, Dordrecht, 1992, Vol. C.

Received December 13, 2013